17th World Conference on Earthquake Engineering, 17WCEE
Sendai, Japan - September 13th to 18th 2020

NON-RESIDENTIAL SINGLE-STORY OLDER STEEL BUILDINGS: EFFECTS OF DESIGN OPTIONS AND ENVELOPE PANELS ON SEISMIC FRAGILITY

G. Cantisani [1], G. Della Corte [2]

[1] *Ph.D. Student, University of Naples Federico II, Napoli, Italy, gaetano.cantisani@unina.it*
[2] *Associate Professor, University of Naples Federico II, Napoli, Italy, gaetano.dellacorte@unina.it*

Abstract

The paper describes a study that is part of an Italian research project (named RINTC), which is addressed to assess the seismic reliability of existing structures made of RC, masonry or steel. Within the project, among the case studies non-residential single-story steel buildings were selected and analyzed by the authors of this paper. First, the design of the steel buildings was simulated according to structural codes and standards of practice used in Italy in the 1980s-1990s. Different structural systems were generated starting from the same structural layout, consisting of five trussed portals in the transverse direction and concentric braces in the longitudinal direction. The main differences between the case studies were in (i) column base and (ii) truss-to-column connections for the portal frames in the transverse direction, (iii) brace cross section and (iv) brace connections for the longitudinal direction. 3D non-linear finite element models were built in OpenSees. Analyses were carried out including or excluding envelope panels from the structural model. This paper describes first results, comparing the structural response for different types of connections in the portal frame direction. Furthermore, the paper presents relevant collapse fragility curves, emphasizing the effect of envelope panels.

Keywords: Collapse, Connection, Fragility, Stability, Steel

1. Introduction

Non-residential single-story steel buildings (SSBs) are generally made by means of moment resisting (portal) frames (transverse direction) and bracing systems (longitudinal direction). The structural system can be varied by changing the connections, thus generating different load paths under both gravity and horizontal actions. Older steel structures are frequently characterized by partial-strength connections, exposing the whole system to premature failure with smaller deformation capacity if compared with modern code-conforming structures. Besides, the type of connection failure can lead to different non-linear behavior depending on the available ductility. In addition, considerations regarding the connection stiffness (typically neglected in the design phase) are also an important aspect of the assessment process, significantly influencing the seismic demands. Besides, strength assignments are usually governed by non-seismic loads and/or geometrical limitations (e.g., slenderness limitations). This originates over-strength relative to seismic design requirements, an aspect that might also significantly affect the seismic vulnerability and consequent economic loss assessment [1, 2]. Considering all these issues, the aim of this work is to quantify the seismic structural response of alternative structural systems that are typically adopted for older SSBs. The main objective of the work is to provide collapse fragility curves. The work is framed within the activity of a broader research project, the ReLUIS-DPC project named RINTC, aimed at evaluating the seismic reliability of structures in Italy with emphasis on ultimate failure [3, 4]. The paper firstly describes the selected case studies. The archetype SSBs were designed according to structural codes and standards of practice used in Italy in the 1980s-1990s [5, 6, 7], considering three different building sites that were agreed upon within the RINTC project. Second, the paper focuses on some of the case studies, describing modeling and analysis. Non-linear static and dynamic response analyses were carried out, including also the effect of cladding panels. Comparisons among the analyzed case studies were carried out and collapse fragility curves were generated, tracing conclusions about implications of the design options and emphasizing the benefits from the cladding and roofing panels.

2. Case study structures

2.1 General description

Figure 1(a) depicts the main geometric characteristics and structural schemes adopted for the archetypes. The generic archetype comprises five main portal frames with truss beams in the transverse (X-) direction. In the longitudinal (Y-) direction, concentric braces provide stiffness and resistance against vertical and horizontal loads. In order to stabilize the upper truss chords, roof braces were used. Longitudinal braces were also used to stabilize the bottom chord members where design actions generated compressive axial forces. Figure 1(a) highlights also the building envelope panels and their openings. Figure 1(b) shows the considered structural schemes. In the transverse direction, two alternatives were selected: (i) a continuous column for the whole height of the building with a pinned column base and a truss beam providing moment action. (ii) A nominally fixed column base and a nominally pinned truss-to-column connection. The first case study will be indicated by the acronym PCB (pinned column base). The second case will be referred to as a “semi-continuous column base” (SCB) because analysis revealed a semirigid and partial strength connection. In the longitudinal direction, two shape of member cross sections and two types of connections were selected for the vertical brace elements: (i) hollow square cross sections and welded gusset plate connections (HSS); (ii) closely spaced built-up angle sections with bolted gusset plate connections (2L). Three building sites were considered, varying seismic hazard from low (Milano, Italy), through medium (Napoli, Italy), to high (L’Aquila, Italy). Table 1 summarizes the selected case studies providing also information on the current work progress: all the case studies were completely designed, and those located at L’Aquila were also statically analyzed; dynamic analysis was also carried out for the PCB-HSS case. In Table 1, the underlined characters highlight the case studies whose analysis is fully discussed in this paper. The allowable stress method was used for designing the structure, assuming the use of the older “Fe 430” steel (nominal yielding strength f_y = 275 *MPa*, nominal ultimate strength f_u = 430 *MPa*, allowable stress σ_a=190 *MPa*).

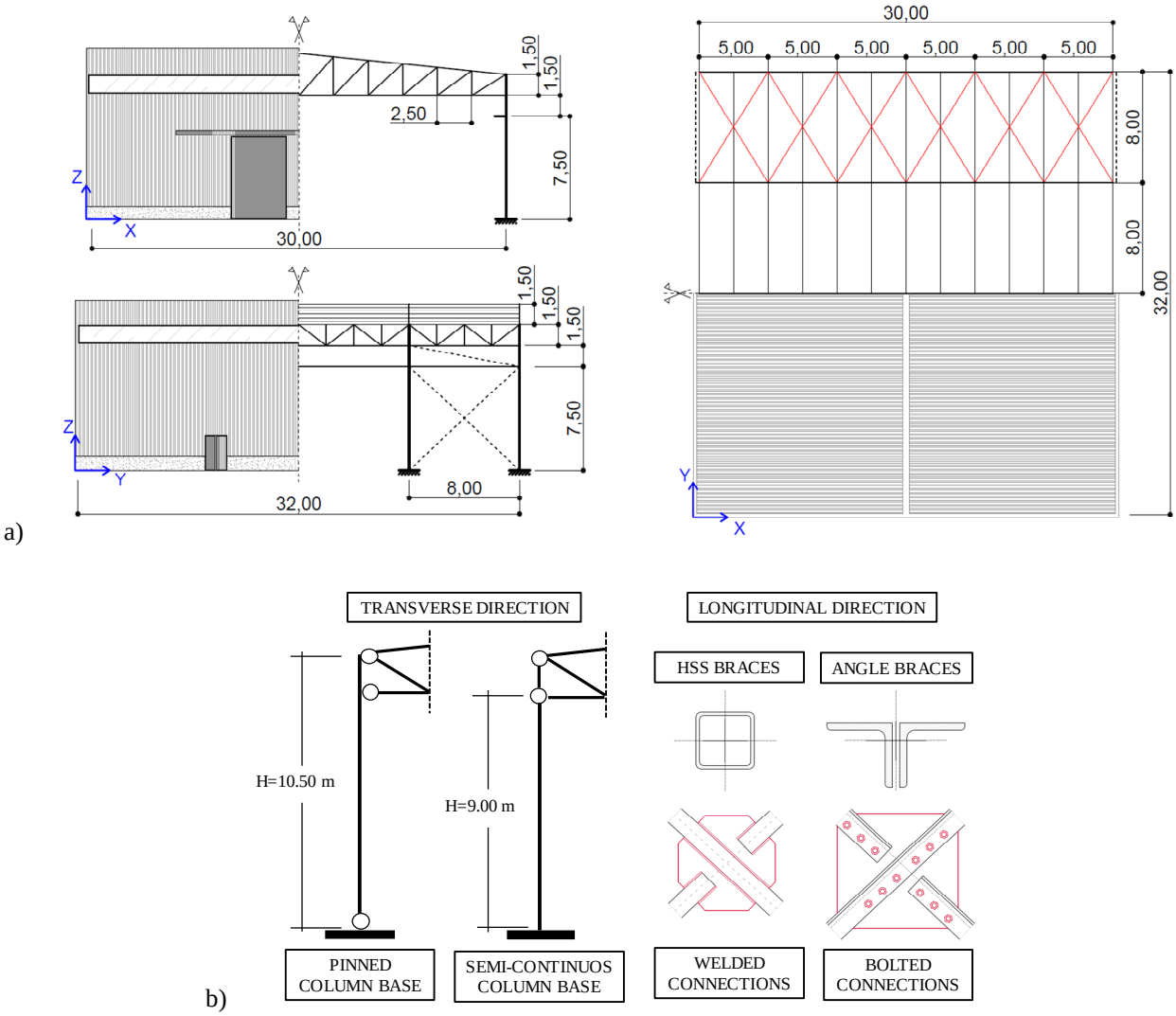

Fig. 1 – (a) Archetype buildings; (b) Structural schemes

Table 1 – Overall view of the RINTC research project for non-residential single-story steel structures

Site	PCB-HSS	PCB-2L	SCB-HSS	SCB-2L
Milano	D	D	D	D
Napoli	D	D	D	D
L'Aquila	D | SA | DA	D | SA	D | SA	D | SA

Legend: D = Designed | SA = Static Analysis | DA = Dynamic Analysis

2.2 Member design

Two load combinations were considered in the design phase: (i) a gravity load combination and (ii) a lateral load combination (considering either wind or seismic loads). Truss member cross sections were chosen to fulfill resistance checks due to gravity loads, while column cross sections were chosen to fulfill deformability checks due to horizontal (wind) loads. As one can see in Figure 2, differences in truss members and column cross sections were obtained for the different structural schemes. The design of the

longitudinal bracing was governed by a brace global slenderness limitation (≤ 200). Consequently, the same brace cross sections were considered for both the PCB and SCB cases. More detailed information concerning the member design and other geometrical dimensions can be found in [8].

2.3 Connection design

Figure 2 shows differences in truss-to-column connections between the PCB and SCB cases. In the PCB case (Figure 2(a)), the connection design was governed by the gravity load combination. In the SCB case, the column cross section was interrupted at 9.00 *m*. From this level, the truss elements were bolted together by means of gusset plates (Figure 2(b)). As shown in the Figure, an end-plate truss-to-column connection was then designed considering the eccentricity arising from the geometry. Figure 2(c) shows the brace-to-column connections in the longitudinal direction: braces were welded to gusset plates, whilst horizontal chord members were bolted.

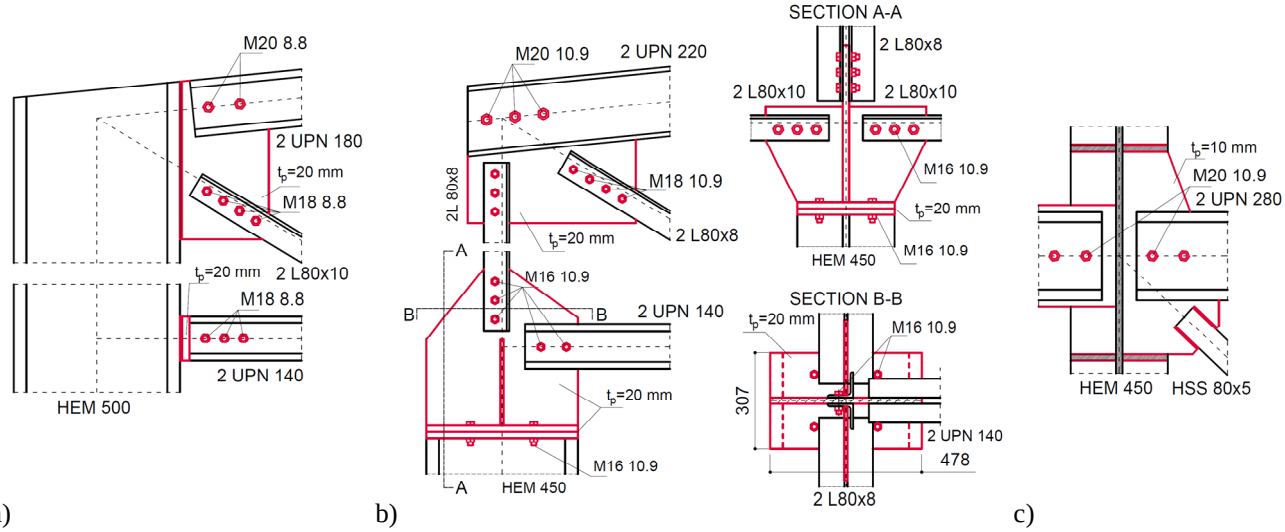

Fig. 2 – Transverse truss-to-column connections: (a) PCB case and (b) SCB case; (c) Longitudinal bracing connections

Figure 3(a) and Figure 3(b) show differences in column base connections between the PCB and SCB cases, respectively. A pinned connection design required four anchor bolts. The anchors were designed to stabilize the column during the erection phases. The steel material used for the anchors was the same (Fe 430) adopted for plates and members. In the SCB design, six anchor bolts were selected for bending moment and shear force resistance. Both gravity and lateral load combinations affected the column base connection design. Base plate stiffeners were added, according to a typical design choice in Italy [9]. No checks in terms of rotational stiffness were made in the design phase. Global deformability checks were carried out considering a perfect rotational restraint provided by the column base connection. However, after designing the connection, the classification criteria stipulated by EN 1993-1-8 [10] were considered. Actually, the column base connection shown in Figure 3(b) is a semi-continuous one, which justifies the acronym (SCB).

2.3 Envelope design

Two alternative types of lateral cladding were considered: (i) sandwich panels (SPs) connected by means of bolts (Figure 4(a)); (ii) trapezoidal sheeting (TS) connected by means of screws (Figure 4(b)). This choice was made to consider non-structural components with significantly different structural behavior. The cladding panels were designed as simply supported beams subjected to horizontal wind actions on the single panel. For the roofing panels, a single trapezoidal sheeting was always considered (completed on-site with thermal insulation and weather shield). The design of the roofing panels was also carried out considering a

simply supported beam between consecutive purlins. Resistance and deformability checks were carried out for both wind and gravity loads.

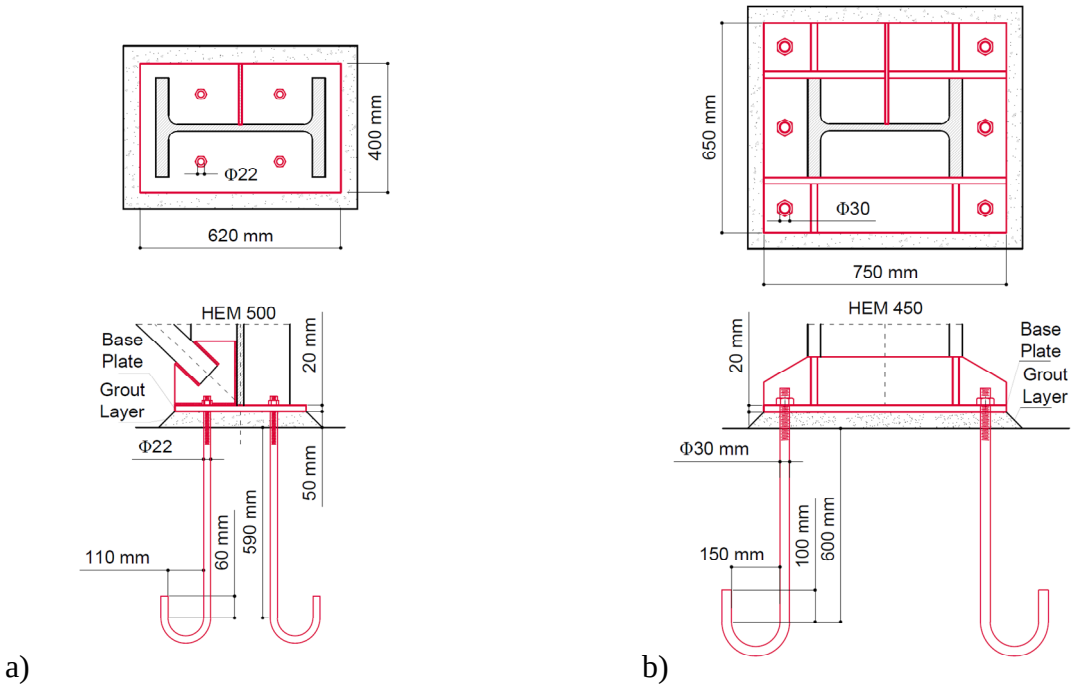

Fig. 3 – Column base connections: (a) PCB case; (b) SCB case.

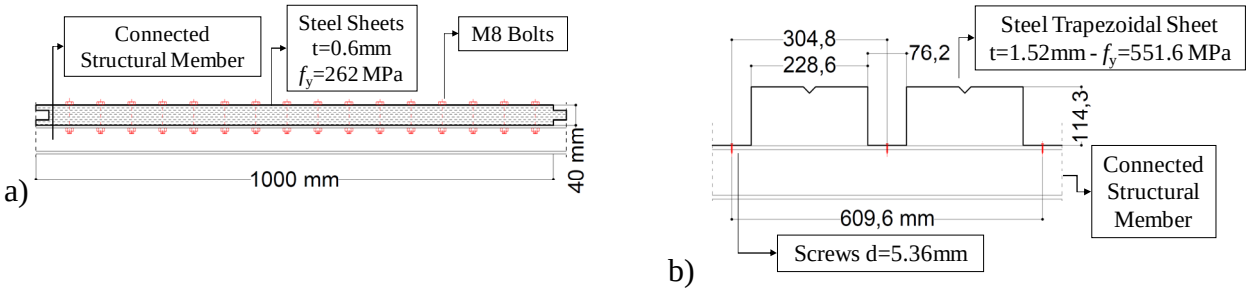

Fig. 4 – (a) Sandwich panel; (b) Trapezoidal sheeting.

3. Non-linear modelling

3.1 General aspects

The archetypes were modelled and analyzed by means of the open-source finite element (FE) software "OpenSees" [11]. The steel stress-strain relationship was characterized by the following parameters: (i) Young modulus E_s = 210 *GPa* and Poisson ratio v = 0.30; (ii) yielding strength f_y = 316 *MPa*, ultimate strength f_u = 479 *MPa* and ultimate strain ε_u = 34% [12]; (iii) post-elastic kinematic hardening ratio E_p = 0.01E_s. In OpenSees, the *Steel02* uniaxial material model was used to simulate the stress-strain relationship. A classical Rayleigh damping model was adopted, with a damping ratio set equal to 5% for two main vibration modes in the two main building directions, as described in Cantisani *et al.* [13]. Columns were modelled as elastic beam-column elements because preliminary analyses indicated that connection and brace failures anticipated column yielding or buckling.

3.2 PCB structure modelling

In the FE model of the PCB case, the non-linear behavior of truss-to-column connections was explicitly represented. The connection shear stiffness and plastic resistance were evaluated according to [10]. The ductility of the bolts in shear was evaluated according to the indications provided by Henriques *et al.* [14]. Figure 5(a) shows schematically the model used for all the truss members. In the longitudinal direction, the non-linear axial and shear force interaction at the column base connections was considered by modelling a single equivalent anchor using a force-based distributed plasticity element with fiber-discretized cross section. Besides, non-linear springs were used to model the circular anchorage in tension and concrete in compression [1]. The model is depicted in Figure 5(b). All the braces were modelled by means of force-based distributed plasticity elements with fiber-discretized cross sections. Equivalent geometrical imperfections were explicitly represented with a sinusoidal shape. The amplitudes of the imperfections were evaluated to obtain the same buckling capacity calculated by means of Eurocode 3 rules [15], using mean values of material strengths and unit values of safety factors. Brace fracture was assessed by implementing the model proposed by Hsiao *et al.* [16]. Accordingly, the local strain range in the brace member was checked until fracture occurred, then propagation of fracture was simulated. Fracture was triggered by a maximum strain range (MSR) value. Therefore, triggering of fracture is generally a function of the loading history. To assess brace fracture in the non-linear static analysis, two alternative MSR capacity values were considered: (i) MSR_1 = half of the capacity according to [16], to consider the case of an ideal symmetric dynamic response in terms of MSR; (ii) MSR_2 = the capacity according to [16], to consider the case of a monotonic loading response. Further details concerning the FE model can be found in Cantisani *et al.* [1].

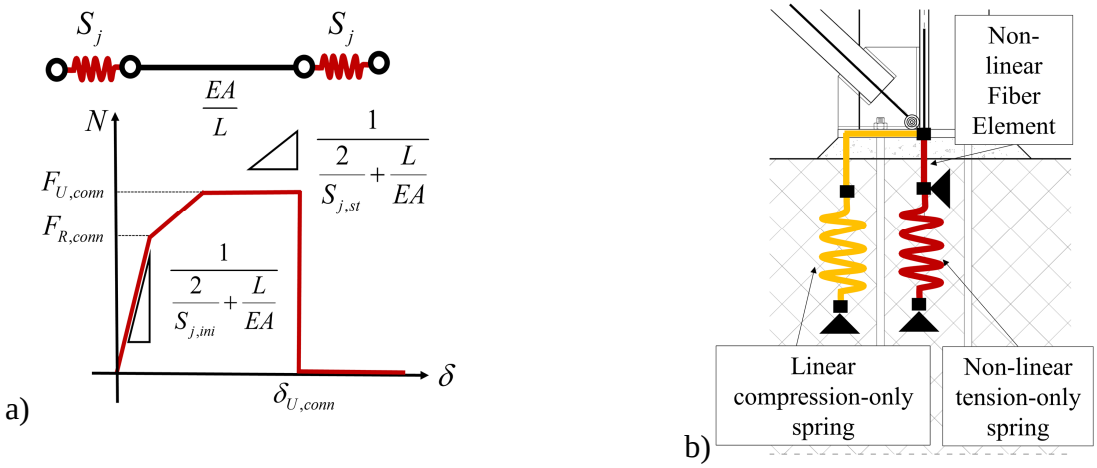

Fig. 5 – Connection modelling for the PCB case: (a) truss-to-column connections; (b) column base connections.

3.3 SCB structure modelling

In the FE model of the SCB case, the non-linear behavior in the transverse direction was concentrated at the semi-continuous column base connection. The method proposed in Della Corte *et al.* [17, 18] was applied in modelling the plastic resistance and rotational stiffness of the connection, assuming a constant axial force produced by gravity loads. The ultimate connection rotation was obtained from the experimental results provided in [19], where one of the column base specimens was very close to the one adopted in this case study, in terms of both connection geometry and anchor details (failure of the connection was reached with anchor fracture after significant bending of the base plate). Additional experimental test results on column base connection cyclic response [20, 21] report ultimate rotation capacities larger than the one assumed in this work. The connection ultimate moment resistance was estimated considering the ultimate axial force resistance developed in one of the anchors (the central one, which is the first yielding anchor in the specific case study). Figure 6(a) shows an example of monotonic and cyclic moment (M_j) vs. rotation (θ_j)

relationship, assuming a perfectly pinched response in modelling the cyclic behavior of the component. This model was chosen as preliminary and the simplest to implement. In the longitudinal direction, all the braced frame connections were explicitly modelled. For example, Figure 6(b) shows the axial force (F_j) vs. axial deformation relationship (δ_j) for the horizontal chord member bolted connections (Figure 2(c)). The plastic resistance and elastic stiffness were evaluated using the component method [10]. The ultimate deformation capacity was evaluated according to the experimental and numerical study described in Može & Beg [22].

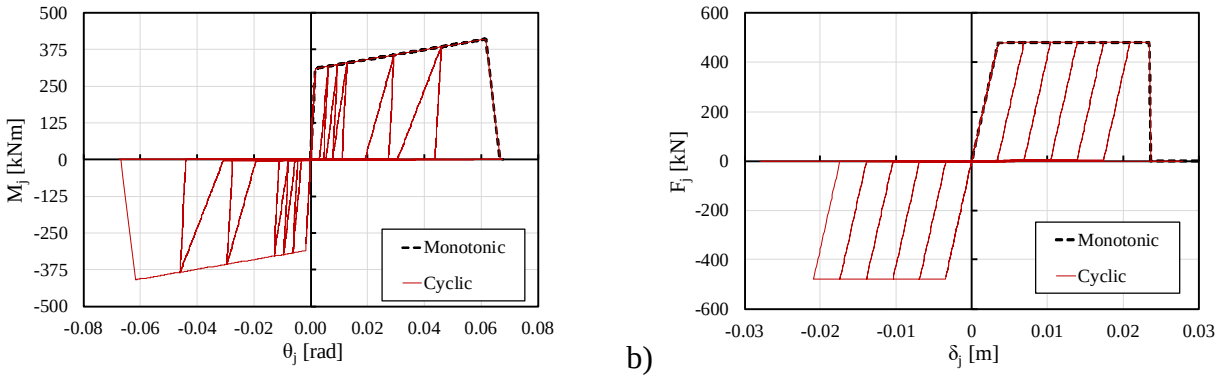

Fig. 6 – Connection modelling for the SCB case: (a) column base connections; (b) bracing chord member connections.

Brace elements were modelled as previously described for the PCB model. Imperfect geometry and mechanical non-linearity were included also in the bottom chord members of the longitudinal trusses. Differently from the PCB case, buckling of longitudinal trusses was expected for two main reasons: (i) the column cross section was interrupted at 9.00 *m*, originating larger axial forces transmitted by the braces to the longitudinal trusses; (ii) yielding of column base connection reduced the axial forces in the PCB longitudinal trusses. Because of buckling of some truss members, adjacent members were subjected to increased tension forces and yielding of the corresponding gusset plate connections occurred. Therefore, the gusset plates connecting the longitudinal truss members were explicitly modelled according to indications provided by Sen *et al.* [23]. Truss-to-column connections were modelled with moment-rotation relationships in both the transverse and longitudinal building directions. The component method [10] was used to estimate the plastic moment resistance and rotational stiffness. No hardening was considered.

3.4 Cladding and roofing panel modelling

Figure 7(a) shows the cyclic response of sandwich panels with bolted connections (SP). The model simulates the experimental response reported in [24]. Such response was characterized by failure of bolted connections between the panel and the secondary steel members.

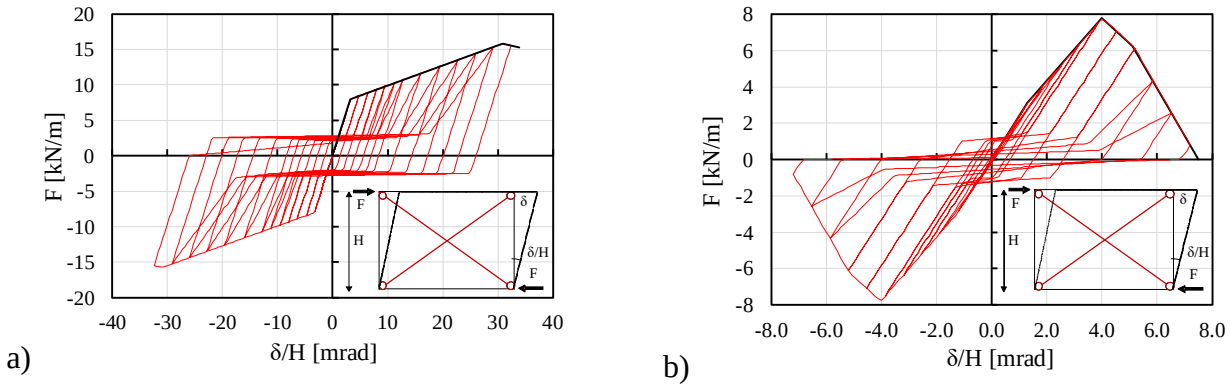

Fig. 7 – Envelope panel modelling: (a) Sandwich panels; (b) Trapezoidal sheeting.

Figure 7(b) shows the cyclic response of the trapezoidal sheeting (TS). The model simulates the experimental response reported in [25], characterized by failure of the screw connections. The procedure described by Cantisani and Della Corte [26] was applied to approximate the actual non-linear response within a multilinear backbone curve. Figure 7 also shows the implemented equivalent diagonal model for a generic sub-assemblage. In fact, secondary steelwork members, as well as connections between side rails and columns, were included in the model [1]. Currently, these modelling strategies were implemented only for the PCB case (labelled as PCB-SP and PCB-TS).

4. Analysis results

4.1 Non-linear static analysis results

Non-linear static (pushover) analyses were preliminarily conducted. Figure 8(a) and Figure 8(b) show pushover results for the bare frame models, respectively for the transverse and longitudinal directions. The structural responses are shown in terms of base shear force ($V_{B,X}$ - $V_{B,Y}$) vs roof displacement (d_X/H, d_Y/H; H = 10.50 m). The roof displacement was evaluated at the joint on the roof aligned vertically with the origin of the coordinate reference system (Figure 1(a)).

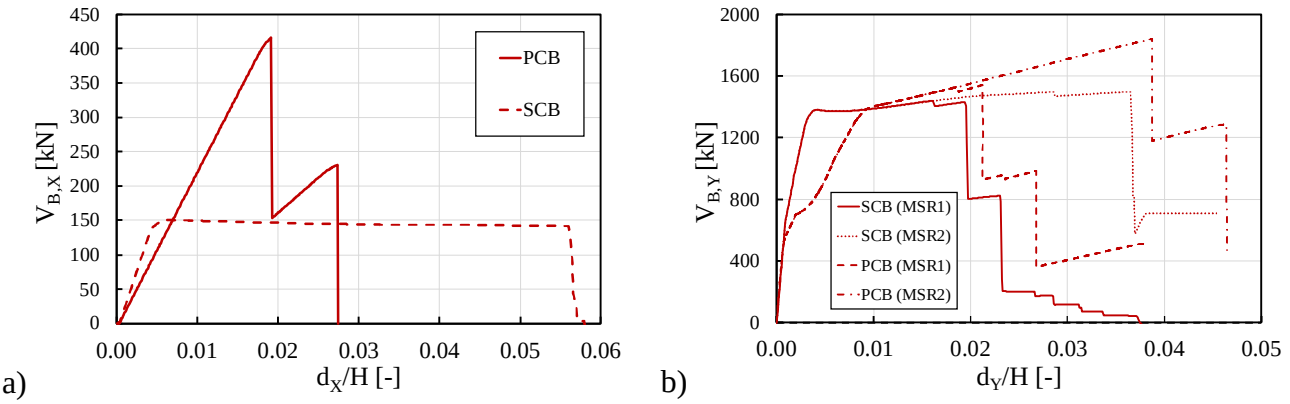

Fig. 8 – PCB vs SCB pushover analysis results: (a) transverse direction; (b) longitudinal direction.

In the transverse direction (Figure 8(a)), the PCB structure shows a brittle structural behavior due to truss-to-column connection failures at both truss ends. Instead, the SCB model shows a ductile behavior provided by yielding of column base connections. Slight P-Delta effect can also be seen in this case. However, the SCB structure appears much less resistant than the PCB case (almost 3 times). In fact, the design of the PCB truss-to-column connections was governed by the gravity load combination, while the lateral load combination governed the design of the SCB column base connections. Consequently, smaller seismic overstrength was obtained in the SCB case compared with the PCB case. In the longitudinal direction (Figure 8(b)), the PCB connections show early yielding due to combined axial and shear forces transmitted by the braces. Ductility and strain hardening of anchors allowed brace yielding and subsequent brace fracture (MSR_1) at a drift equal to 2.7%. For the PCB case and after brace fracture, a secondary moment frame action took place and the lateral resistance did not drop to zero. In the PCB-MSR_2 case, brace fracture is delayed at a drift equal to d_Y/H=3.9% but anchor fracture occurred first at a drift equal to d_Y/H=2.6% (anchor fracture was not explicitly modelled). The SCB model shows the same PCB initial lateral stiffness. However, in the SCB case, column base connections were strong enough to allow brace yielding first. Looking at the MSR_1 assumption, triggering the brace fracture implies the lateral resistance reducing to zero (d_Y/H=2.0%). In fact, no secondary moment frame action took place in this case, because the truss-to-column connection plastic resistance was developed at a preceding step in the pushover analysis. The same structural behavior appears looking at the MSR_2 case, but with a delay in brace fracture. No drift limitations due to column base connection failure were observed in the SCB model. Differences in drift values associated with brace fracture can be seen between the PCB and SCB models, for both the MSR_1 and MSR_2 assumptions. Such

differences were mainly due to the anticipated yielding of the column base connections in the PCB model. Such plastic deformations of column base connections increased the drift capacity in the PCB case.

Within the RINTC research project [3], a drift corresponding to a 50% drop in the base shear force resistance was assumed to correspond with the global collapse of the building. For the purpose of this study, in the PCB case, collapse assessment was carried out also considering a drift corresponding to 100% drop in resistance. These limiting drifts from the pushover response curves were then used to assess structural collapse in the non-linear dynamic analysis, as described in the subsequent section.

4.2 Non-linear dynamic analysis results

Multi-stripe dynamic analyses (MSAs) [27] were carried out considering 20 pairs (X- and Y- components) of ground motions (GMs) per each stripe, simulating bi-directional response. Ten stripes were considered varying the earthquake return period of the seismic actions from 10 *yrs* to 100000 *yrs*. The intensity measure (IM) was the spectral pseudo-acceleration at the first-mode vibration period ($S_a(T_1)$). The GM selection was carried out in order to have pseudo-acceleration spectra with the same S_a from the hazard curve at a given earthquake return period and structure vibration period ([3]). The seismic hazard curves used for this work are reported in Figure 9(a). The two hazard curves consider differences in the main period of vibration (T_X) of the analyzed buildings. Therefore, two GM sets were considered: (i) GM selection considering T=1 s for the PCB bare frame model ($T_{X,PCB}$ = 1.06 *s*); (ii) GM selection considering T=0.5 s for both the PCB-SP and PCB-TS models ($T_{X,PCB\text{-}SP}$ = 0.54 *s* – $T_{X,PCB\text{-}TS}$ = 0.54 *s*). Portal frame peak drift demands ($d_{X,peak}/H$) are plotted in Figure 9(b), Figure 9(c) and Figure 9(d), respectively for the PCB, PCB-SP and PCB-TS case.

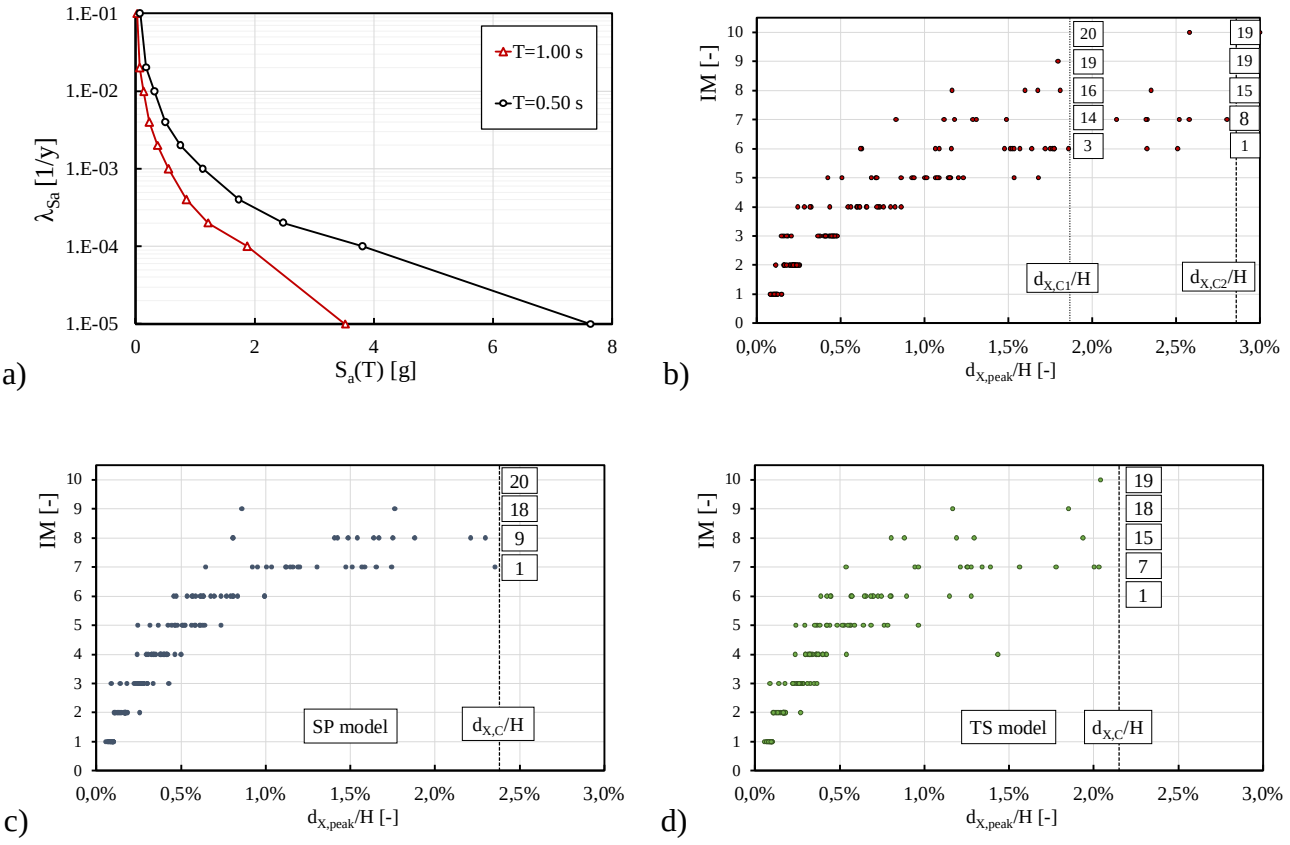

Fig. 9 – MSA results: (a) Hazard curves; (b) PCB model; (c) PCB-SP model; (d) PCB-TS model.

In fact, in all the considered cases, the transverse direction was the weakest building direction, i.e., collapse was almost always due to failure of connections in the portal frames. Brace fracture was reached in the last analysis stripe (IM = 10, T_R = 100000 *yrs*) for a small number of GMs (1 GM for the PCB model, 2 GMs for

the PCB-SP model and 3 GMs for the PCB-TS model). Anchor fracture never occurred. The figures also show the number of collapse cases corresponding to each IM value (numbers highlighted in the text boxes within the plots in Figure 9). Results show that collapse cases started from IM = 6 (i.e., T_R= 1000 *yrs*) for both the PCB and the PCB-TS cases. IM = 7 (i.e., T_R= 10000 *yrs*) started collapse cases in the PCB-SP structure (Figure 9(c)). Statistical evaluations and local component responses are discussed in [4].

5. Collapse fragility curves

5.1 Main assumptions and methodology

Collapse fragility functions were built using the peak maximum demand-to-capacity ratio for the entire (3D) structure. To represent fragility, a lognormal probability distribution function was chosen. Estimates of the mean and standard deviation (i.e., $\hat{\eta}$ and $\hat{\beta}$) were obtained using the freely available software described in [28]. The approach takes into account uncertainties in the estimation of the lognormal distribution parameters, by deriving an approximate distribution of $\hat{\eta}$ and $\hat{\beta}$ by means of a parametric resampling of the number of failure cases given by the MSA results. Therefore, mean and standard deviation of both $\hat{\eta}$ and $\hat{\beta}$ were obtained and numerical values are reported in Figure 10.

5.2 Fragility curves

The fragility curves for the PCB case are plotted in Figure 10(a). The hazard curve (Figure 9(a)) was that corresponding to $S_a(T = 1\ s)$. The median S_a value varied from 0.80 *g* to 0.97 *g* when the collapse criteria varied from 50% to 100% loss in lateral resistance. Correspondingly, the expected standard deviation varied from 0.42 to 0.34. Figure 10(a) shows also fragility curves for the structural models including the envelope panels. In this case, the hazard curve (Figure 9(a)) was that corresponding to $S_a(T = 0.5\ s)$. Cladding by TS led to the worse structural response, compared to the same structure but with cladding made of SPs. In fact, the median S_a value varied from 2.07 *g* to 2.69 *g*, respectively for the TS and SP cases. In Figure 10(a), the plot shows also the ratio of the number of collapse cases (obtained by summing the number of collapse cases in both X- and Y- directions) to the total number of analysis runs. The ratios are reported as circles or triangles in the plots. It is worthy noting that the fragility curves always fitted well the points corresponding to the observed collapse cases. This is also confirmed quantitatively by the small dispersions in the estimated values of both β and η ($\max(\sigma_\beta)$ = 0.07, $\max(\sigma_\eta)$ = 0.07). To highlight the benefits from including the cladding panels in the fragility evaluation, Figure 10(b) shows the conditional probability of collapse given T_R, corresponding to each of the 10 values of the earthquake return periods considered for the hazard curve (Figure 9(a)). Results clearly show that structural models including envelope panels (i.e., PCB-SP and PCB-TS models) provided a probability of collapse always smaller than the corresponding bare frame model. For instance, for T_R = 2500 *yrs* the probability of collapse reduced from 0.56 (PCB-50%) to 0.06 (PCB-SP).

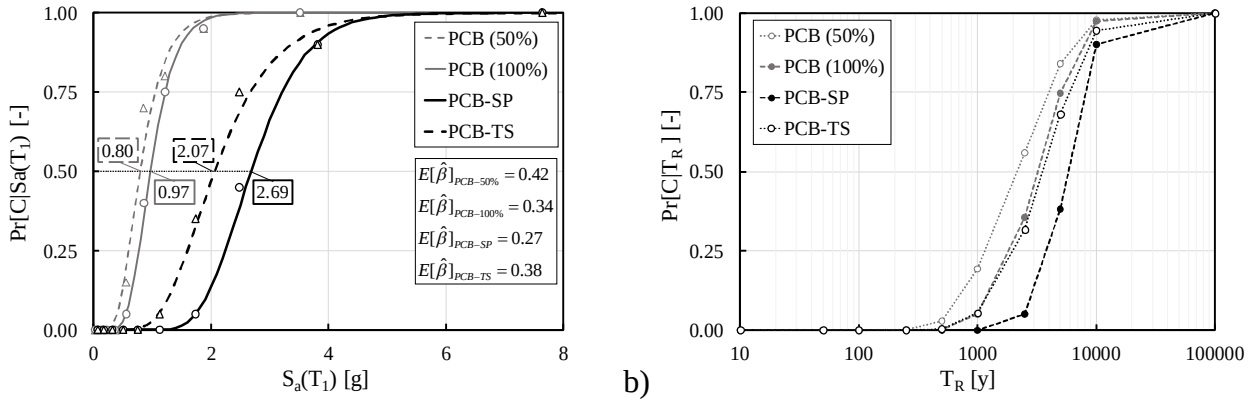

Fig. 10 – (a) Collapse fragility curves; (b) Conditional probability of collapse given T_R.

6. Conclusions

The paper presented results from an ongoing research study on collapse assessment of older non-residential single-story steel buildings. Assumptions in the structural layout of case studies were presented and discussed. Three archetypes were analyzed using non-linear static and dynamic response assessment. Results show that connection failure led to the structural collapse of the buildings in all the examined cases. (i) The bare frame structure with pinned column base (PCB) connections was governed by the brittle shear failure of truss-to-column connections. The lateral drift capacity corresponding to zero lateral shear resistance in the pushover analysis was equal to 2.9%. The median $S_a(T_1)$ leading to collapse was 0.97 g, from the dynamic analysis. (ii) The bare frame structure with a semi-continuous column base (SCB) connections was governed by a more ductile column base connection failure. The lateral drift capacity corresponding to zero lateral shear resistance in the pushover analysis was equal to 5.7%. However, the lateral resistance of the SCB structure was almost 3 times smaller than the PCB case. Non-linear dynamic analyses have been planned for this case and they are currently under investigation. (iii) The effect of envelope panels on fragility was assessed for the PCB archetype by explicitly modelling two cladding types: (a) a relatively strong and ductile sandwich panel assembled by means of bolted connections (SP); (b) a relatively weak and brittle trapezoidal sheeting assembled by means of screw connections (TS). In terms of fragility, the median $S_a(T_1)$ varied from 2.06 g (building with TS) to 2.69 g (building with SPs). The conditional probability of collapse, given the earthquake return period, always reduced when the structural model included explicitly the envelope panels. Future development of the study will be addressed to assess fragility by: (i) including envelope effects also in the SCB configuration; (ii) changing the brace section and connections.

7. Acknowledgements

Support of the ReLUIS consortium and the Italian Department of Civil Protection (DPC) is acknowledged.

8. References

[1] Cantisani G., Della Corte G., Sullivan T.J. and Roldan R. (2020): Displacement-Based Simplified Seismic Loss Assessment of Steel Buildings, *Journal of Earthquake Engineering* (accepted for publication).

[2] Cantisani G., Della Corte G. (2019): Simplified Displacement-Based Economic Loss Assessment of Single-Storey Steel Buildings. *Proceedings of SECED Conference on Earthquake Risk and Engineering towards a Resilient World*, Greenwich, England.

[3] Iervolino, I., Spillatura, A., Bazzurro, P. (2019): RINTC-E project: towards the assessment of the seismic risk of existing structures in Italy. *Proceedings of the 7th ECCOMAS Thematic Conference on Computational Methods in Structural Dynamics and Earthquake Engineering*, Crete, Greece.

[4] Cantisani G., Della Corte G. (2019): RINTC-E: Seismic risk of pre-code steel single-story non-residential buildings in Italy. *Proceedings of the 7th International Conference on Computational Methods in Structural Dynamics COMPDYN 2019 (paper ID 19971)*, 24-26 June, Crete, Greece.

[5] CS.LL.PP. C 24 Maggio, Istruzioni relative ai carichi, ai sovraccarichi ed ai criteri generali per la verifica di sicurezza delle costruzioni. Gazzetta Ufficiale della Repubblica Italiana, 140, 1982.

[6] CS.LL.PP. (1986): DM 24 Gennaio, Norme tecniche per le costruzioni in zone sismiche. *Gazzetta Ufficiale della Repubblica Italiana*, 108.

[7] CNR – Consiglio Nazionale delle Ricerche (1988): Costruzioni di acciaio: Istruzioni per il calcolo, l'esecuzione, il collaudo e la manutenzione, *CNR-UNI 10011*.

[8] Cantisani G, Della Corte G. (2018): Seismic response of non-conforming single-story non-residential buildings considering envelope panels. *Proceedings of the 9th International Conference on Advances in Steel Structures (p.p. 1725-1736), 5-7 December*, Hong Kong, China.

[9] Della Corte G, Iervolino I, Petruzzelli F (2013): Structural modelling issues in seismic performance assessment of industrial steel buildings. *Proceedings of the 4th ECCOMAS Thematic Conference on Computational Methods in Structural Dynamics and Earthquake Engineering*, Kos Island, Greece.

[10] CEN (2009): EN 1993-1-8: Eurocode 3: design of steel structures—part 1–8: Design of joints. *European Committee for Standardization*, Brussels, Belgium.

[11] McKenna, F., Scott, M. H., and Fenves, G. L. (2010): Nonlinear Finite-Element Analysis Software Architecture Using Object Composition. *Journal of Computing in Civil Engineering*, **24**(1), 95-107.

[12] Badalassi, M., Braconi, A., Cajot, L.-G., Caprili S., et al. (2017): Influence of variability of material mechanical properties on seismic performance of steel and steel-concrete composite structures. *Bulletin of Earthquake Engineering*, **15**, 1559-1607.

[13] Cantisani G, Della Corte G., Landolfo R. (2018): Modelling and analysis of an archetype non-residential old steel building for collapse risk evaluation. *Proceedings of the 16th European Conference on Earthquake Engineering (paper ID 10180), 18-21 June*, Thessaloniki, Greece.

[14] Henriques, J., Jaspart, J.P., Da Silva, L.S. (2014): Ductility requirements for the design of bolted lap shear connections in bearing. *Advanced Steel Constructions*, **10**(1), 33-52.

[15] CEN (2005): EN 1993-1-1: Design of steel structure – part 1-1: General rules and rules for buildings. *European Committee for Standardization*, Brussels, Belgium.

[16] Hsiao, P.C., Lehman, D.E, Roeder, C.W. (2012): A model to simulate special concentrically braced frames beyond brace fracture. *Earthquake Engineering & Structural Dynamics*, **42**, 183-200.

[17] Della Corte G., Cantisani G., Landolfo R. (2017): Seismic response of built-up steel columns with semi-continuous base-plate connections. *Proceedings of the Eight European Conference on Steel and Composite Structures (Eurosteel 2017)*, September 13-15, Copenhagen, Denmark.

[18] Della Corte G., Cantisani G., Landolfo R. (2018): Battened Steel Columns with Semi-Continuous Base Plate Connections: Experimental Results vs. Theoretical Predictions. *Key Engineering Materials*, **763**, 243-250.

[19] Della Corte, G, Landolfo, R. (2017): Lateral loading tests of built-up battened columns with semi-continuous base-plate connections. *Journal of Constructional Steel Research*, **138**, 783-798.

[20] J.E. Grauvilardell, D. Lee, J.F. Hajjar, R.J. Dexter (2005): Synthesis of design, testing and analysis research on steel column base plate connections in high seismic zones. *Structural Engineering Report No. ST-04-02, Department of Civil Engineering*, University of Minnesota.

[21] Gomez I., Kanvinde A., Deierlein G. (2010): Exposed column base connections subjected to axial compression and flexure. *Final Report Presented to the American Institute of Steel Construction (AISC)*.

[22] Može P., Beg D. (2014): A complete study of bearing stress in single bolt connections. *Journal of Constructional Steel Research*, **95**, 126-140.

[23] Sen A., Roeder C.W., Lehman D.E., Berman J.W. (2019): Nonlinear modelling of concentrically braced frames. *Journal of Constructional Steel Research*, **157**, 103-120.

[24] De Matteis G., Landolfo R. (1999): Structural behaviour of sandwich panel shear walls: An experimental analysis. *Material and Structures*, **32**, 331-341.

[25] O'Brien P., Eatherton M.R., Easterling W.S. (2017): Characterizing the load-deformation behavior of steel deck diaphragms using past test data. *Cold-Formed Steel Research Consortium Report Series, CFSRC R-2017-02*.

[26] Cantisani G., Della Corte G. (2019): In-Plane Shear Force-Displacement Modelling of Steel Trapezoidal Sheeting. *Proceedings of 4th International Workshop on the Seismic Performance of Non-Structural Elements*, Pavia, Italy.

[27] Jalayer, F. and Cornell, C. A. (2009): Alternative non-linear demand estimation methods for probability-based seismic assessments. *Earthquake Engineering & Structural Dynamics*, **38**(8), 951–972.

[28] Baraschino R, Baltzopoulos G, Iervolino I. (2020): R2R-EU: Software for fragility fitting and evaluation of estimation uncertainty in seismic risk analysis. *Soil Dynamics and Earthquake Engineering* (accepted for publication).

